HHS Public Access

Author manuscript

Dev Cell. Author manuscript; available in PMC 2016 July 27.

Published in final edited form as:

Dev Cell. 2015 July 27; 34(2): 229–241. doi:10.1016/j.devcel.2015.06.021.

A Synthetic Niche for Nephron Progenitor Cells

Aaron C. Brown, **Sree Deepthi Muthukrishnan**, and **Leif Oxburgh***

Center for Molecular Medicine, Maine Medical Center Research Institute, 81 Research Drive, Scarborough, ME 04074

Summary

FGF, BMP and WNT balance embryonic nephron progenitor cell (NPC) renewal and differentiation. By modulating these pathways we have created an *in vitro* niche in which NPCs from embryonic kidneys or derived from human embryonic stem cells (hESCs) can be propagated. NPC cultures expanded up to a billion-fold in this environment can be induced to form tubules expressing nephron differentiation markers. Single-cell culture reveals phenotypic variability within the early CITED1-expressing NPC compartment indicating that it is a mixture of cells with varying progenitor potential. Furthermore, we find that the developmental age of NPCs does not correlate with propagation capacity, indicating that cessation of nephrogenesis is related to factors other than an intrinsic clock. This *in vitro* nephron progenitor niche will have important applications for expansion of cells for engraftment and will facilitate investigation of mechanisms that determine the balance between renewal and differentiation in these cells.

Graphical Abstract

*Corresponding author: oxburl@mmc.org.

Author contributions

A.C.B. and L.O. designed research; A.C.B. and S.D.M. performed research; A.C.B., S.D.M. and L.O. analyzed data; and A.C.B. and L.O. wrote the paper.

Supplementary Figures

Supplementary material includes 7 figures, 1 table and a detailed experimental protocol.

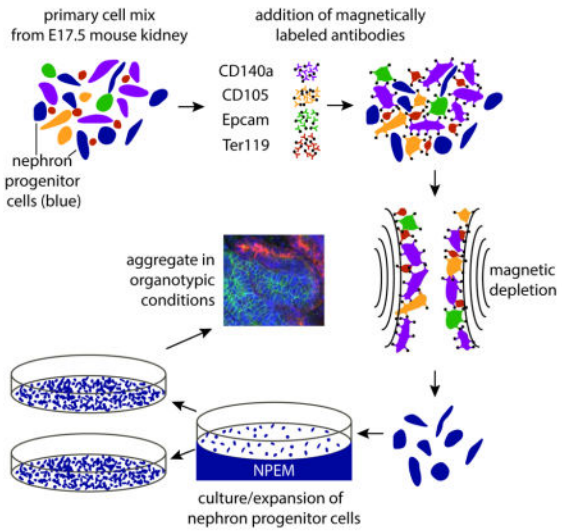

Introduction

The nephron is the filtering unit of the kidney and is essential for regulating blood urea concentration and limiting water and electrolyte loss. New nephron formation is limited to the fetal period in humans and continues to postnatal day 4 (P4) in rodents. The mature mouse kidney lacks an identifiable population of multipotent nephron stem cells and is not thought to replace entire nephrons after they are lost, although replacement of damaged cells within tubules does occur (Humphreys et al., 2008; Rinkevich et al., 2014). Thus, long-term organ function relies on nephron over-capacity, which is determined during the fetal/postnatal period (Little and Bertram, 2009). Urea excretion can be augmented by dialysis, but transplantation is eventually required for patients with severe organ impairment. End-stage renal disease affects approximately 500,000 individuals in the United States and organ availability does not match demand (Abdel-Kader et al., 2009). Technology for *ex vivo* nephrogenesis would enable therapeutic replacement of damaged kidney tissue, and rapid advances in reprogramming somatic cells to the pluripotent state and differentiating these through the intermediate mesoderm lineage to nephron progenitor cells (NPCs) have brought the prospect of generating patient-specific human kidney tissue within reach (Lam et al., 2014; Mae et al., 2013; Taguchi et al., 2014; Takahashi and Yamanaka, 2006; Takasato et al., 2014). While these proof-of-principle experiments have elegantly shown differentiation of NPCs, procedures to expand these progenitors will be necessary for practical applications such as engraftment (Lam et al., 2014; Takasato et al., 2014).

The mammalian kidney develops by radial addition of new nephrons that form at the outer most cortex within a progenitor cell niche known as the nephrogenic zone. As the collecting duct branches, progenitor cell aggregates at the collecting duct tips known as cap mesenchymes are induced to differentiate into renal vesicles, polarized derivatives that are the earliest precursors of the epithelial components of the nephron (Mori et al., 2003). The continuous epithelial induction of NPCs causes their depletion, necessitating a mechanism to balance progenitor cell renewal with epithelial differentiation, enabling multiple rounds of

nephrogenesis. Focus on this question has led to the discovery of distinct cell phenotypes, or compartments, that comprise the cap mesenchyme and the specific signaling pathways on which these cells depend (Figure 1A) (Brown et al., 2013; Kobayashi et al., 2008; Mugford et al., 2009; Park et al., 2012).

The least differentiated NPC compartment is marked by the transcriptional co-activator CITED1 and the transcription factor SIX2 (known as the CITED1+ compartment) (Boyle et al., 2008; Self et al., 2006). SIX2 expression is necessary to prevent NPCs from differentiating prematurely, but no functional role has been described for CITED1 and in our studies it is simply used as a marker for the least differentiated compartment within the cap mesenchyme (Boyle et al., 2007; Self et al., 2006). Previous studies by our group and others have identified essential functions of the BMP, FGF, and WNT signaling pathways in regulating the balance between renewal and differentiation in these cells (Barak et al., 2012; Blank et al., 2009; Brown et al., 2011a; Brown et al., 2013; Carroll et al., 2005; Karner et al., 2011). We asked if our understanding of the signaling environment for NPCs is sufficient to allow its reconstruction by manipulation of reported signaling pathways *ex vivo*. CITED1+/SIX2+ cells were used in a screening strategy to combinatorially test the potential of known nephrogenic zone signaling pathways to promote NPC renewal. We show that CITED1+/SIX2+ cells can be propagated in an undifferentiated state, yet retain the potential for epithelial differentiation. Furthermore, these conditions can be extrapolated to hESC-derived NPCs. Overall, we have used a predictive approach to functionally recapitulate conditions in the nephrogenic zone to expand undifferentiated yet functionally competent NPCs that can be used for nephron regeneration experiments.

Design

We are interested in understanding early events in development of the mammalian nephron, with the ultimate goal of recapitulating nephrogenesis *in vitro* using defined cell populations. To date, we have not had access to pure NPCs in the quantities required for experimentation. Therefore, the goal of this study was to develop an *in vitro* environment in which NPCs could be propagated in an undifferentiated state, as they are in their biological niche within the embryonic kidney. Several published studies have characterized the signaling environment of the embryonic NPC niche, the nephrogenic zone (Barak et al., 2012; Blank et al., 2009; Brown et al., 2011a; Brown et al., 2013; Carroll et al., 2005; Karner et al., 2011). For this reason we chose a directed approach to recapitulate the signaling environment of the nephrogenic zone in culture.

Results

SMAD inhibition retains NPCs in the CITED1-expressing compartment

As a starting point for the development of conditions for propagation of NPCs, we made use of observations on signaling in cap mesenchyme during the terminal stage of nephrogenesis. We have previously shown that BMP7 signaling through the SMAD1/5 pathway is required for undifferentiated CITED1+/SIX2+ progenitors to transition to a CITED1−/SIX2+ state in which they are sensitized to epithelial induction by WNT/β-catenin signaling (Figure 1A) (Brown et al., 2013). Cessation of nephrogenesis is defined as the final round of new

nephron formation in which the last wave of NPCs undergoes mesenchyme to epithelial transition. In the mouse this occurs shortly after birth and is accompanied by a reduction in *Cited1*+ cap mesenchyme by P2 (Figure 1B) (Hartman et al., 2007; Rumballe et al., 2011). We reasoned that SMAD1/5 signaling might increase during the terminal phase of nephrogenesis, skewing the renewal versus differentiation balance and depleting the cap mesenchyme. Immunostaining of mouse kidneys from E17.5 to P2 for activated SMAD1/5 (pSMAD1/5) showed that this is indeed the case, and that an expanded domain of SMAD1/5 activation in many cap mesenchymes associates with cessation of nephrogenesis (Figure 1C).

To understand if cap mesenchyme cells in their natural signaling environment could be prevented from transitioning out of the native CITED1+ progenitor cell state, we treated newborn animals with the SMAD1/5 small molecule inhibitor LDN-193189 (LDN) during the first two postnatal days. LDN is highly specific for SMAD1/5 and has been successfully used *in vivo* (Yu et al., 2008). Immunoblot of isolated nephrogenic zone cells (NZCs) from LDN-treated animals demonstrates greater than 95% reduction in SMAD1/5 phosphorylation compared to controls (Figure 1D). To measure the differentiation status of NPCs, we used the *Cited1creERT2-EGFP* and *Six2cre-EGFP* mouse strains, which dynamically express fluorescent protein under the control of *Cited1* and *Six2* promoters (Boyle et al., 2008; Kobayashi et al., 2008). While untreated animals lost expression of *Cited1* and *Six2* in cap mesenchyme at P2 and P3, respectively, expression was maintained in LDN-treated pups (Figure 1E). RT-qPCR analysis of isolated nephrogenic zone cells with additional marker genes that are expressed within these two compartments supports the conclusion that the progenitor state had been rescued in LDN-treated cap mesenchymes (Figure 1F). We observed expression of CITED1+/SIX2+ compartment-specific transcripts such as *Cited1*, *Meox1* and *Six2* and loss of markers for the CITED1−/SIX2+ and pretubular aggregate (PTA) compartments, including the WNT/β-catenin response genes *Wnt4*, *Lef1* and *Sp5*. Transcription of BMP response genes including Crossveinless-2 (*Cv2*) and several Inhibitors of differentiation (*Ids*) was also decreased, consistent with suppression of SMAD signaling by LDN (Figure 1F). Kidneys of treated mice aged for two weeks after the LDN administration are slightly larger and contain more nephrons than vehicle-treated controls as determined by counting glomeruli in serial kidney sections spaced 100 μm apart (Figure 1G and 1H). Although less precise than counting all glomeruli using stereology, this index is proportional to the number of glomeruli, and nephrons, in each kidney. We conclude that inhibition of pSMAD1/5 activation can retain cap mesenchyme cells in a *Cited1*+/*Six2*+ progenitor cell state within their natural signaling niche and that this pharmacological delay of CITED1+ depletion results in increased nephron endowment.

To understand if these observations can be extrapolated to CITED1+ cells in culture, we performed a series of experiments on NPCs isolated from embryonic mouse kidneys. Using our previously developed isolation protocol, CITED1+ NPCs were harvested from embryonic kidneys between the ages of E13.5 to P1 at near 100% purity, allowing interrogation of the CITED1+ population at multiple time points (Figure 2A and 2B) (Brown et al., 2013). However, CITED1 progenitor purity drops to 75% by P2, likely due to the loss of CITED1+ progenitors that occurs during cessation (Figure 1B and Figure 2B).

When aggregated on polycarbonate filters at the air-liquid interface and cultured in serum free medium (aggregate cultures) in the presence of the WNT/β-catenin agonists BIO (2 μM) or CHIR99021 (CHIR, 3 μM), these progenitors undergo robust tubulogenesis, which is dependent on endogenously produced BMP ligand (Brown et al., 2013; Osafune et al., 2006). CITED1+ progenitors isolated from P0 *Cited1creERT2-EGFP* mice underwent tubulogenesis and lost GFP expression by day 4 of CHIR treatment (Figure 2C). However, addition of LDN blocked tubulogenesis and maintained GFP expression. These results demonstrate that pSMAD1/5 inhibition can retain cultured progenitors in an undifferentiated *Cited1*+ state in the presence of active BMP and WNT/β-catenin signaling, suggesting that LDN treatment is key to *in vitro* propagation of these cells.

The developmental regulators FGF, BMP, and WNT are required for maintenance, expansion and differentiation of CITED1+ progenitors

To define additional factors required for NPC propagation in monolayer we made use of prior studies on signaling in cap mesenchyme (Figure 1A and Figure 3A). Addition of FGF1, 2, 9, or 20 promotes the maintenance and proliferation of CITED1+ progenitors when cultured in monolayer on fibronectin coated wells with keratinocyte serum free medium (KSFM) (Brown et al., 2011a). However, these cells lost expression of cap mesenchyme markers after 2 to 3 days and died. We chose to use FGF9 for CITED1 maintenance and proliferation as it was recently identified as a natural ligand for maintenance of NPCs *in vivo* (Barak et al., 2012). Heparin was included as it facilitates the binding of FGF9 to its receptor. We have shown that BMP activation of the JNK pathway is critical for the proliferation of mouse NPCs (Blank et al., 2009). Although NPCs express *Bmp7*, we included recombinant BMPs 4 and 7 to counteract the dilution of endogenous BMP7 in the culture medium. These factors function equivalently in NPC renewal (Oxburgh et al., 2005). WNT signaling is necessary for proliferation and renewal of CITED1+ progenitors (Karner et al., 2011). Since LDN blocks cells from transitioning to the SIX2 only state in which they become sensitive to WNT-mediated epithelialization, we were able to add CHIR (1.25 μM) without promoting differentiation (Brown et al., 2013). The Rho kinase inhibitor Y-27632 was included because it improves survival of dissociated stem cells during plating and passage and supports their long-term maintenance (Tsutsui et al., 2011; Watanabe et al., 2007). Insulin like growth factors 1 and 2 (IGF1/2) were included because they promote cell proliferation, inhibit cell death and are important for kidney growth and nephron endowment in rodents (Bach and Hale, 2015; Rogers et al., 1999). Nephron Progenitor Expansion Medium (NPEM) was formulated by supplementing APEL medium with these factors (Figure 3A). APEL was selected as the basal medium and Matrigel™ as the substrate because they have been used in the derivation of hESC-derived NPCs (Takasato et al., 2014). NPCs isolated from E17.5 kidneys were plated and expanded 16-fold in NPEM and maintained robust expression of the cap mesenchyme markers CITED1, PAX2 and WT1 after 3 days in culture (Figure 3B). Using flow cytometry on E17.5 CITED1+ NPCs derived from *Cited1creERT2-EGFP* mice, we evaluated the requirement for each of the culture additives to maintain cells in monolayer in the undifferentiated state by subtracting them from NPEM (Figure 3C and 3D). NPCs grown in the absence of either FGF9 or BMP4/7 for 3 days failed to expand and displayed a shrunken morphology (Figure 3D and Figure S1A). Cells grown in the absence of IGF1/2 maintained CITED1 expression but cell growth was

restricted compared to complete NPEM. In the absence of the WNT agonist CHIR, cells failed to expand but remained CITED1+ and were indistinguishable from cells grown in complete NPEM (Figure 3C, 3D and Figure S1A). In the absence of the Rho kinase inhibitor Y-27632 there was a significant decrease in cell attachment to the substrate, a corresponding increase in cell-cell contact, and importantly, a large proportion of NPCs transitioned out of the CITED1 compartment (Figure 3D and Figure S1A), demonstrating that inhibition of this pathway plays an important role in maintaining progenitor identity.

When LDN was subtracted from the medium, cells expanded but were largely CITED1 negative (Figure 3B–D). In the absence of LDN, nuclear localization of pSMAD1/5 increased dramatically, as did transcription of the SMAD response gene *Cv2* (Figure 3E and 3F). While NPCs were still competent to undergo tubulogenesis after subtraction of IGF1/2, Y-27632 or CHIR, the absence of LDN rendered cells unable to undergo differentiation after 7 days in aggregate culture as determined by E-cadherin (ECAD) and lotus lectin staining (LTL) (Figure 3G and Figure S1B). In addition to losing CITED1 expression, progenitors cultured in the absence of LDN for 3 days lost expression of characteristic marker genes including PAX2, WT1, and SIX2, which may explain their lack of competence (Figure 3B and Figure S2). These results demonstrate that the SMAD signaling branch of the BMP pathway must be subdued to maintain NPC potential.

Passage and differentiation potential of NPCs grown in NPEM

In this study, the term passage is used to denote detachment, dilution, and replating of cells for propagation. The term doubling is used to describe a two-fold increase in cell number within a population. When grown in NPEM, CITED1+ progenitors isolated from multiple developmental stages including E13.5, E17.5, and P1 maintained expression of CITED1/SIX2 and did not express the PTA marker LEF1 through at least 6 passages when detached and replated (hereafter referred to as “split”) at a constant cell density determined by initial proliferation rate for each developmental time point (Figure 4A–C). A comprehensive protocol for the isolation and culture of NPCs can be found in Supplementary Experimental Procedures. CITED1+ cells proliferated vigorously in NPEM and had undergone 17 to 23 doublings by passage 6 (Figure 4B). CITED1+ progenitors from P1 kidneys retained the ability to expand at greater than 98 percent purity after 2 freeze-thaw cycles and at least 10 passages (Figure 4A–C). CITED1+ progenitors displayed minimal slowing of proliferation over many passages as determined by a consistent time to doubling of cell number (doubling time) (Figure 4D). Interestingly, E17.5 CITED1+ progenitors seeded at a higher cell density (50,000 vs 20,000 per cm^2) and split every 3 days, displayed a substantially decreased doubling capacity after each passage until cells no longer expanded by passage 3, demonstrating a critical need to avoid cellular overgrowth (Figure 4D). We conclude that our attempt to recapitulate the nephrogenic zone signaling environment for progenitor cells successfully allows extensive propagation of undifferentiated cells.

Cessation of nephrogenesis is associated with CITED1+ compartment depletion between P1 and P4, indicating that the differentiation state of NPCs in this phase of nephrogenesis might differ from cells at earlier stages (Figure 1B) (Hartman et al., 2007). The CITED1+ compartment contains domains that may be functionally heterogeneous and a subset that

expresses *Meox1* and *Dpf3* lies adjacent to the differentiating CITED1−/SIX2+ compartment, suggesting that it is poised to differentiate (Mugford et al., 2009). CITED1+ progenitors isolated from P1and E17.5 kidneys show comparable expression of *Cited1* and *Six2*, but P1 cells express higher levels of *Meox1*, suggesting that they may have shifted to a more differentiated state (Figure 4E). Interestingly, P1 progenitors also show increased *Jag1*, which is normally expressed in the renal vesicle. To functionally test the susceptibility of cells from different stages to differentiation we isolated cells from E16.5, E17.5, P1, and P2 in KSFM medium, which does not contain any of the factors we have identified as essential for NPC renewal, treated them with a WNT/β-catenin agonist, and measured *Wnt4*, which is expressed as NPCs differentiate (Figure 4F and (Brown et al., 2013)). While treatment elevated *Wnt4* in P2 progenitors compared to E17.5 and P1, no difference was seen between E17.5 and P1, suggesting that P1 cells purified by our isolation protocol are not yet primed for differentiation (Figure 4F). Thus, although P1 progenitors display a molecular marker signature consistent with a differentiated state within the CITED1+ compartment, they do not show evidence of increased sensitivity to WNT/β-catenin induction and retain the potential to expand over 1 billion fold (30 doublings) (Figure 4B).

To confirm that *in vitro* propagated NPCs retain their differentiation competence, we tested their capacity for epithelial induction by aggregating them and culturing under organotypic conditions at the liquid/air interface of DMEM/F12 medium containing 3 μM CHIR (differentiation medium). Compared to vehicle controls, extensive tubule-like structures were seen by stereomicroscopy in cells from all passages tested (Figure 4A, bottom). Aggregates of E17.5 NPCs that had been expanded and passaged prior to culture in differentiation conditions revealed a marker profile characteristic of nephron differentiation (Figure 5A). This included sequential expression of LEF1 (PTA), ECAD (epithelialization), PAX8 (comma and S-shaped body) and LTL staining (mature proximal tubules). Progenitors isolated from E13.5, E17.5 and P1 that were expanded through multiple passages formed both ECAD+ and LTL+ tubule structures (Figure 5B). In some instances LTL+ tubules were observed that were contiguous with ECAD+ tubules (Figure 5C). Using markers for distal convoluted tubule (NCC) and proximal tubule (LTL) with ECAD we identified three distinct nephron segments in E17.5 kidneys: LTL+/ECAD− (proximal), ECAD+/NCC+ (distal), ECAD+/NCC− (undetermined, presumptive loop of Henle) (Figure 5D). Although abundant proximal and ECAD+/NCC− segments could be identified in aggregates treated with CHIR, we were initially unable to identify NCC+ distal tubules. Recent studies of cell signaling processes that pattern the early nephron have demonstrated that suppressing SMAD1/5 signaling promotes the distal fate (Lindstrom et. al., 2014). Hypothesizing that differentiation fates may be skewed by the culture conditions, we supplemented our differentiation medium with LDN from day 4 to 7. ECAD+/NCC+ tubules became abundant and could clearly be distinguished from adjacent ECAD+/NCC− tubules, confirming that our initial culture conditions inhibited the distal tubule fate (Figure 5E). Thus, expanded CITED1+ progenitors are competent to form tubules with marker profiles of proximal, distal and presumptive intermediate tubule segments.

NPCs isolated from the E11.5 kidney display different signaling requirements compared to those isolated at later developmental stages, prompting us to ask if cells from this stage can

be expanded in NPEM (Brown et al., 2013). 50,000 CITED1+ cells were purified from E11.5 mesenchymes by magnetic depletion and cultured in NPEM on Matrigel. Similar to later developmental stages, LDN was necessary to retain E11.5 NPCs in an undifferentiated state while remaining competent to undergo tubulogenesis (Figure S3). Cells expanded vigorously to one million after only 3 days in culture, but aggregate assays revealed that their capacity for passaging with maintained differentiation capacity was severely restricted compared to NPCs from later stages (Figure S4). The underlying reason for the profound difference in expansion capacity between E11.5 NPCs and cells from later stages remains unclear, and we conclude that NPEM is most useful for progenitor expansion from E13.5 onward.

Clonally expanded NPCs are competent to form nephron tubules

We have demonstrated that bulk populations of pure CITED1+ progenitors can be expanded in NPEM while retaining their potential to undergo differentiation. We next tested a mixed culture of cells isolated from the nephrogenic zone to determine if our culture conditions confer a selective growth advantage to NPCs. An isolation method was used that results in a mixed population of NZCs consisting of approximately 50% NPCs, 35% cortical interstitial cells and 15% other cells with trace contamination of collecting duct cells (Blank et al., 2009; Brown et al., 2011b; Brown et al., 2013). Expansion of a bulk culture of these NZCs in NPEM increased the proportion of SIX2+ cells from 50% to 85% after 2 passages (Figure 6A). Clones of CITED1+ cells expanded after 5 days in a limiting dilution assay using NZCs (Figure 6B). Twenty independent clones were expanded for 8 days and all tested positive for CITED1, SIX2 or PAX2, indicating preferential outgrowth of cells of the NPC lineage (Figure 6B). We conclude that NPCs expand preferentially in NPEM over other cell types found within the nephrogenic zone and that NPC specific clones can be expanded from a single cell using our culture conditions.

Heterogeneity of gene expression suggests that the CITED1+ compartment contains cells with varying degrees of progenitor potential (Mugford et al., 2009). To determine if the CITED1+ compartment represents a homo- or heterogeneous progenitor population, we performed a limiting dilution analysis. 960 cells from a bulk population of E17.5 CITED1+ progenitors were distributed across ten 96 well plates. After attachment, the number of cells seeded per well mirrored the expected Poisson distribution (Figure S5A). Cells in each well were counted and only wells containing single cells were further analyzed. After 5 days, the number of cells per clone was counted to compare the doubling times of individual progenitors (Figure 6C). The growth rate observed was heterogeneous with 10% of clones doubling 7 times (17 hours per average doubling), a rate higher than that seen with our earlier low density seeding of bulk cultures (31.6 hours per average doubling). Wells containing a single colony derived from a single cell that fell within this higher proliferating category were interrogated further to determine their capacity for expansion.

We found that many of the larger colonies started to show increased clustering of cells, which may subject NPCs to overgrowth and restrict growth potential or even cause spontaneous differentiation through increased cell-cell contact. To circumvent this and to expand our clones further, 24 high growth clones were split and passed to 2 wells each,

expanded to confluence and either transferred to aggregate culture for differentiation or immunostained with anti-CITED1 antibody to determine purity. Over half of the clones were greater than 90% CITED1+ and 15 grew to more than 100,000 cells (Figure 6D and S5B). There was a correlation between CITED1 purity and total cell expansion, with the 12 most expanded clones averaging 90% CITED1 purity and the 12 least expanding clones averaging only 60% purity. Several outlier clones (1, 14 and 15) had a lower cell number after the passage and when these cells were placed in aggregate culture, they had a reduced ability to undergo tubulogenesis compared to clones that were still expanding after the passage, suggesting that they might have become compromised (Figure 6E). Of the 24 clones, only 1 did not undergo tubulogenesis (#5), and this clone was associated with the lowest percentage of CITED1+ progenitors (4%). The remaining 23 clones underwent partial to complete tubulogenesis when subjected to differentiating conditions in aggregate culture. One healthy clone was further expanded over a period of 23 days including 2 passages and underwent extensive tubulogenesis when transferred to aggregate (Figure 6F). Confocal microscopy of this clonally derived aggregate showed numerous ECAD and LTL positive tubules with lumens that can be visualized by optical sectioning. Overall, our results provide functional evidence that the CITED1+ compartment is comprised of NPCs that display a wide variability in progenitor potential.

Expansion of functional NPCs derived from hESCs

To understand if cellular growth in NPEM can be directly extrapolated to human cells, we repeated our analysis with NPCs derived from hESCs using a recently published protocol (Takasato et al., 2014). CITED1+/SIX2+/PAX2+/WT1+ cells generated using this procedure lost expression of NPC markers following a single passage (Figure 7A and Figure S6A). However, hESC-derived NPCs could be passaged at least twice (1:8 split) with retained molecular marker expression using our propagation conditions (Figure 7B and Figure S6B). Subtraction of individual components from the medium revealed a critical dependence on FGF9, LDN, CHIR, and Y27632 for expression of CITED1, PAX2, SIX2, and WT1 (Figure S7A). When LDN was eliminated from the medium during the passage 2 culture, cells lost expression of PAX2 (Figure 7C). When BMP4/7 was removed, PAX2 and SIX2 expression remained robust, whereas CITED1 was decreased and WT1 was eliminated (Figure S7A). Interestingly, when both BMP4/7 and LDN were removed concurrently, PAX2 expression remained, suggesting that LDN is only necessary to retain marker expression in the presence of exogenous BMP (Figure S7B).

To evaluate the functional capacity of expanded human NPCs, we differentiated cell aggregates from each passage. Very few tubules formed from cells expanded during passages 0 and 1 in either medium, although the tubules that did form stained positive for LTL (Figure 7E). In contrast, cells cultured through passage 2 in NPEM underwent robust differentiation forming many tubules containing lumens (Figure 7E and 7F). We found staining for both ECAD and LTL in differentiated tubules and observed that tubules frequently expressed both of these markers (Figure 7G). When found in tubules without ECAD, LTL staining was confined to the luminal side of tubules, where it normally stains L-fucose present on the surface of the microvilli that form the brush border. This suggests that these tubules have increased surface area, which is necessary for the resorptive and flow

sensing functions of proximal tubules *in vivo*. We also observed persistent nuclear expression of PAX8, which is normally expressed in proximal and distal convoluted tubules and loops of Henle in humans, but is decreased or absent in adult mouse kidneys (Figure 7H and (Tong et al., 2009)). PAX8 staining also shows alternating expression intensity in neighboring cells within a tubular structure, similar to that observed in human proximal tubules (Tong et al., 2009). In tubules co-expressing both markers, LTL often overlapped with ECAD staining at cell-cell junctions, but displayed stronger expression towards the luminal side (Figure 7G). Since this pattern was only found in ECAD positive tubules, and ECAD expression is normally decreased prior to terminal differentiation of the proximal tubule in mice and rats, these structures may represent immature tubules where microvilli have not yet formed and in which expression of these two markers has not yet segregated. Another possibility is that the immediate precursors to proximal and distal tubule epithelial cells (LTL−/ECAD+) have become intermixed and given rise to a number of hybrid tubules within the organoid culture, rather than becoming regionally restricted to a single tubule type. Overall, we have demonstrated that NPEM expands ES cell derived human NPCs that are capable of robust epithelialization and formation of tubules with lumens that display expression of markers normally associated with human proximal tubules.

Discussion

We have shown that the nephrogenic zone cell signaling environment can be recreated *in vitro* for extensive propagation of undifferentiated NPCs. Modulation of FGF, BMP, WNT and ROCK signaling pathways was necessary to maintain cells in the CITED1+ state with epithelial differentiation potential. This defined culture system can be used to expand embryonic mouse NPCs and hESC-derived NPCs for *in vitro* organogenesis studies. Cell signaling requirements for mouse and human NPCs are similar in all aspects except the requirement for BMP. Subtraction of BMP from the culture medium of human cells resulted in only a partial loss of the progenitor marker profile compared to the complete loss observed for mouse progenitors. Published differentiation protocols for hESCs generate at most 50% NPCs, and approximately half of the culture remains undefined (Lam et al., 2014; Mae et al., 2013; Takasato et al., 2014). It therefore seems likely that cells in the culture may be producing BMPs and other factors that mask the effects of BMP7 withdrawal. Development of purification procedures for human NPCs will be necessary to directly compare the signaling requirements of derived human NPCs with CITED1+ cap mesenchyme cells.

Limitations of the NPC culture procedure

The experimental procedure for isolation and propagation of NPCs that we describe is of limited use at the earliest stages of nephrogenesis prior to E13.5, and at terminal stages of nephrogenesis after P1. However, we show that E13.5, E17.5 and P1 NPCs proliferate vigorously in NPEM. Two key steps of the procedure are particularly sensitive to error. First, the initial enzymatic digestion of the nephrogenic zone to liberate NPCs and other niche cells must be performed correctly. Insufficient removal of the kidney capsule leads to a very low starting cell number because few cells are liberated. Conversely, damaging the kidney during the dissection will expose regions below the nephrogenic zone and reduce the

proportion of NPCs in the cell suspension, making the magnetic depletion step less efficient. Second, it is critical to control the density of NPC growth. NPCs will begin to spontaneously differentiate when crowded, severely limiting the passaging potential of the culture. Cultures must be split when the most crowded zone on the culture plate reaches 70 % – 80 % density (Supplementary Experimental Procedures).

BMP signaling in NPC maintenance

FGF, BMP and WNT each influence renewal and differentiation of the NPC, but how the cell interprets these signals depends on its differentiation state as well as concurrent signaling from the surrounding niche (Brown et al., 2013; Das et al., 2013; Fetting et al., 2014; Karner et al., 2011). BMP7 promotes NPC proliferation through a MAPK pathway, whereas pSMAD signaling transitions progenitors out of the CITED1+ compartment (Blank et al., 2009; Brown et al., 2013). Molecular mechanisms that determine the balance of MAPK versus pSMAD activation by BMP7 in NPCs are not understood. However, recent data suggests that FGF signaling through PI3K/MAPK may repress pSMAD1/5 signaling in unprimed cap mesenchyme (Motamedi et al., 2014). In our cultures, pSMAD1/5 persists in the presence of exogenously added FGF9, suggesting that additional niche factors present in the developing organ are required for FGF-mediated suppression of pSMAD in the CITED1+ compartment. A key factor in the development of our culture procedure was the addition of the small molecule LDN, which blocks pSMAD activity and prevents progenitors from exiting the CITED1+ compartment, while still allowing proliferation and survival signals provided by BMP stimulation.

Functional heterogeneity within the CITED1+ progenitor population

Gene expression profiling of the CITED1+ cap mesenchyme suggests that this is not a homogenous cell population (Mugford et al., 2009). *Meox1* and *Dpf3* are expressed in a specific subpopulation of CITED1+ progenitors adjacent to the more differentiated CITED1−/SIX2+ compartment and are not expressed in CITED1+ progenitors in more cortical cap mesenchyme. While the functions of these transcription factors during kidney development are unknown, their localized expression indicates that the CITED1+ population may be phenotypically heterogeneous, perhaps with one renewing sub-compartment, and one sub-compartment in the process of exiting the CITED1+ state. Our analysis of single cells cultured for 5 days revealed a largely binomial distribution of cellular doubling, supporting functional heterogeneity of the CITED1+ cap mesenchyme population. Clones derived from the most rapidly dividing group could be expanded to several hundred thousand cells that retained the potential for epithelial differentiation. It seems probable that these highly proliferative clones derive from cells within the CITED1+ compartment with extensive progenitor potential that might function as “super progenitors” from which the bulk of CITED1+ cap mesenchyme cells are derived. Lineage analysis using a tamoxifen-inducible *Cited1-creERT2;Rosa26RLacZ* strain shows that a high proportion of cells labeled at E13.5 are retained in the cap mesenchyme at E19.5, suggesting the presence of a self-renewing sub-population (Boyle et al., 2008). An alternate possibility is that our medium formulation provides an advantage to more differentiated cells within the CITED1+ compartment. Single cell transcriptome analysis coupled with phenotyping of a large

number of cap mesenchyme cells will be required to discern the biological basis for the heterogeneity that we see within the CITED1+ population.

The nephrogenic niche regulates NPC lifespan

Recent high resolution studies indicate that cap mesenchyme displays progressively decreased proliferation and thinning throughout development until it is depleted (Short et al., 2014). Based upon this model and the average cell cycle lengths calculated for the cap mesenchyme (33 hours at E17.25), E17.5 progenitors in the CITED1+ compartment would on average be expected to expand no more than 2 doublings prior to cessation. However, in isolation, differentiation-competent E17.5 CITED1+ progenitors were able to double 17 times starting either as bulk populations or single cells. Surprisingly, CITED1+ progenitors isolated at P1 underwent more than 30 doublings in bulk culture. If progenitor renewal was internally regulated by a predetermined biological clock that counts the number of divisions, we would not expect cells isolated from E17.5 and P1 to double more than twice. Instead, bulk cultures of progenitors from E13.5, E17.5 and P1 proliferate and expand similarly, suggesting that signals limiting replicative lifespan of these cells are provided by their environment. Based on this we speculate that the reduced speed of proliferation of P1 progenitors *in vivo* may underlie their depletion, perhaps because epithelial induction by collecting duct tips is not reduced proportionally, leading to cap mesenchyme exhaustion. We cannot rule out the possibility that a specific factor in the medium resets a biological clock in NPCs that limits proliferation potential. Further screening to compare the effect of medium components on cells isolated from different stages of nephrogenesis will be required to definitively answer this question.

Conclusions

This work demonstrates that our understanding of the nephrogenic zone signaling environment is now sufficiently advanced to allow us to emulate the niche *in vitro*, providing a means for controlled expansion of NPCs. These cells can now be produced in large quantities facilitating studies of nephron formation in a variety of biological matrices with the ultimate goal of tissue engraftment.

Experimental procedures

A detailed protocol for the isolation and propagation of NPCs can be found in Supplementary Experimental Procedures.

Cell culture

CITED1+ progenitors were purified from NZCs derived from E17.5 mouse kidneys as previously described (Brown et al., 2011b; Brown et al., 2013). CITED1+ progenitors were cultured in monolayer on hESC-qualified Matrigel-coated plates (Corning). Population doublings for each cell passage were calculated in Microsoft Excel using the log base 2 formula, =LOG(N1,2)-LOG(N0,2), where 2 represents log base 2, N1 is the final cell count at the end of a passage and N0 is the initial seeding density at the start of a cell passage. To derive NPCs from human ES cells, H9 ES cells were dissociated with TrypLE, washed in autoMACs running buffer and plated at 10,000 cells per cm^2 on Matrigel-coated 96-well

plates in APEL medium supplemented with 10 μM Y-27632. The following day cells the medium was changed to APEL medium containing 8 μM CHIR99021. After 48 hours cells were exposed to APEL medium containing 200 ng/ml FGF9 and 1 μg/ml heparin for 4 days. For hESC-derived NPCs grown in NPEM, the medium was then changed to NPEM for 4 days (end of pass 0). Cells grown in NPEM were subsequently passaged 1:8 upon 100% confluence for future passages and medium was changed every 2 days. For passaging of human and mouse NPCs, cells were dissociated by incubation with TrypLE (Life Technologies) for 2 minutes at 37°C, washed and spun 2X at 300g in autoMACs running buffer (Miltenyi) prior to resuspension in NPEM as described in Figure 3A. NPEM is changed every 2 days. The human H9 ES cell line (WiCell) was used at passages 31–33 and derived as previously described (Amit et al., 2000). Cells were differentiated in aggregate culture with 3 μM CHIR99021 (Stemgent) in medium as previously described (Brown et al., 2013).

Immunofluorescence and microscopy

Tissue sections, monolayer cultures and aggregates were immunostained as previously described (Blank et al., 2009; Brown et al., 2013). Antibodies were used at 1:100 dilution and include CITED1 (NeoMarkers); pSMAD1/5 (Cell Signaling Technology); SIX2 (Proteintech); LEF1 (Cell Signaling Technology); PAX2 (Proteintech); PAX8 (Proteintech); ECAD (BD Transduction Laboratories), NCC (Millipore) and LTL staining at 1:200 (Vector Laboratories). Live images of GFP+ progenitors from *Cited1creERT2-EGFP* mice in monolayer or aggregate culture were imaged with epi-fluorescent and fluorescent stereo microscopes, respectively.

Quantitative PCR

RNA purification, cDNA synthesis, and quantitative PCR were performed as described in (Brown et al., 2011a). Raw data are normalized to β-actin expression, and fold changes are relative to the vehicle control. Primer sequences are listed in Supplementary Experimental Procedures.

Flow cytometry

CITED1+ progenitors were purified from GFP+ kidneys isolated from *Cited1creERT2-EGFP* x ICR mice and cultured as described in the text. GFP fluorescence intensity and cell counts were collected on a FACSCalibur (BD) and data were analyzed using FlowJo software.

Statistical methods

For qPCR, kidney weights and glomerular counts, P-values shown were calculated using a two-tailed Student's t-test and $P<0.05$ was considered significant. Error bars for qPCR experiments represent standard deviation (±SD) for technical replicates derived from NZCs of 20–24 pooled kidneys or standard error (±SE) for biological replicates derived from 3 independent mouse litters of pooled kidneys (Figure 4E and F). For flow cytometry and cell count experiments, error bars represent average values ±SD calculated from three culture well replicates. CITED1+ purity was determined from at least 3 independent images by

normalizing to the number of DAPI-stained nuclei in each field using ImageJ with error bars representing the mean ±SD.

Mouse strains and treatments

Animal care was in accordance with the National Research Council Guide for the Care and Use of Laboratory Animals and protocols were approved by the Institutional Animal Care and Use Committee of Maine Medical Center. CITED1 progenitors were derived from kidneys of *Cited1creERT2-EGFP* x ICR heterozygous mice. *Cited1creERT2-EGFP* and *Six2cre-EGFP* mouse strains are maintained on an FVB/NJ background (Boyle et al., 2008; Kobayashi et al., 2008). Pregnant mice were injected at 12 hour intervals at the times indicated with 3 mg/kg LDN-193189 in 20 μl of DMSO/PBS.

Supplementary Material

Refer to Web version on PubMed Central for supplementary material.

Acknowledgments

This work was supported by National Institutes of Diabetes and Digestive and Kidney Disease (NIDDK) Grant R01DK078161 (LO) and Department of Defense Grant PR110346 (LO). Core facilities support was provided by Maine Medical Center Research Institute core facilities for Molecular Phenotyping and Progenitor Cell Analysis (supported by National Institutes of General Medicine (NIGM) 8P30 GM106391) and Histopathology (NIGM 5P30 GM106391 and 5P30 GM103392).

References

Abdel-Kader K, Unruh ML, Weisbord SD. Symptom burden, depression, and quality of life in chronic and end-stage kidney disease. Clin J Am Soc Nephrol. 2009; 4:1057–1064. [PubMed: 19423570]

Amit M, Carpenter MK, Inokuma MS, Chiu CP, Harris CP, Waknitz MA, Itskovitz-Eldor J, Thomson JA. Clonally derived human embryonic stem cell lines maintain pluripotency and proliferative potential for prolonged periods of culture. Dev Biol. 2000; 227:271–278. [PubMed: 11071754]

Bach LA, Hale LJ. Insulin-like growth factors and kidney disease. Am J Kidney Dis. 2015; 65:327–336. [PubMed: 25151409]

Barak H, Huh SH, Chen S, Jeanpierre C, Martinovic J, Parisot M, Bole-Feysot C, Nitschke P, Salomon R, Antignac C, et al. FGF9 and FGF20 maintain the stemness of nephron progenitors in mice and man. Dev Cell. 2012; 22:1191–1207. [PubMed: 22698282]

Blank U, Brown A, Adams DC, Karolak MJ, Oxburgh L. BMP7 promotes proliferation of nephron progenitor cells via a JNK-dependent mechanism. Development. 2009; 136:3557–3566. [PubMed: 19793891]

Boyle S, Misfeldt A, Chandler KJ, Deal KK, Southard-Smith EM, Mortlock DP, Baldwin HS, de Caestecker M. Fate mapping using Cited1-CreERT2 mice demonstrates that the cap mesenchyme contains self-renewing progenitor cells and gives rise exclusively to nephronic epithelia. Dev Biol. 2008; 313:234–245. [PubMed: 18061157]

Boyle S, Shioda T, Perantoni AO, de Caestecker M. Cited1 and Cited2 are differentially expressed in the developing kidney but are not required for nephrogenesis. Dev Dyn. 2007; 236:2321–2330. [PubMed: 17615577]

Brown AC, Adams D, de Caestecker M, Yang X, Friesel R, Oxburgh L. FGF/EGF signaling regulates the renewal of early nephron progenitors during embryonic development. Development. 2011a; 138:5099–5112. [PubMed: 22031548]

Brown AC, Blank U, Adams DC, Karolak MJ, Fetting JL, Hill BL, Oxburgh L. Isolation and culture of cells from the nephrogenic zone of the embryonic mouse kidney. J Vis Exp. 2011b

Brown AC, Muthukrishnan SD, Guay JA, Adams DC, Schafer DA, Fetting JL, Oxburgh L. Role for compartmentalization in nephron progenitor differentiation. Proc Natl Acad Sci U S A. 2013; 110:4640–4645. [PubMed: 23487745]

Carroll TJ, Park JS, Hayashi S, Majumdar A, McMahon AP. Wnt9b plays a central role in the regulation of mesenchymal to epithelial transitions underlying organogenesis of the mammalian urogenital system. Dev Cell. 2005; 9:283–292. [PubMed: 16054034]

Das A, Tanigawa S, Karner CM, Xin M, Lum L, Chen C, Olson EN, Perantoni AO, Carroll TJ. Stromal-epithelial crosstalk regulates kidney progenitor cell differentiation. Nat Cell Biol. 2013; 15:1035–1044. [PubMed: 23974041]

Fetting JL, Guay JA, Karolak MJ, Iozzo RV, Adams DC, Maridas DE, Brown AC, Oxburgh L. FOXD1 promotes nephron progenitor differentiation by repressing decorin in the embryonic kidney. Development. 2014; 141:17–27. [PubMed: 24284212]

Hartman HA, Lai HL, Patterson LT. Cessation of renal morphogenesis in mice. Dev Biol. 2007; 310:379–387. [PubMed: 17826763]

Humphreys BD, Valerius MT, Kobayashi A, Mugford JW, Soeung S, Duffield JS, McMahon AP, Bonventre JV. Intrinsic epithelial cells repair the kidney after injury. Cell Stem Cell. 2008; 2:284–291. [PubMed: 18371453]

Karner CM, Das A, Ma Z, Self M, Chen C, Lum L, Oliver G, Carroll TJ. Canonical Wnt9b signaling balances progenitor cell expansion and differentiation during kidney development. Development. 2011; 138:1247–1257. [PubMed: 21350016]

Kobayashi A, Valerius MT, Mugford JW, Carroll TJ, Self M, Oliver G, McMahon AP. Six2 defines and regulates a multipotent self-renewing nephron progenitor population throughout mammalian kidney development. Cell Stem Cell. 2008; 3:169–181. [PubMed: 18682239]

Lam AQ, Freedman BS, Morizane R, Lerou PH, Valerius MT, Bonventre JV. Rapid and efficient differentiation of human pluripotent stem cells into intermediate mesoderm that forms tubules expressing kidney proximal tubular markers. J Am Soc Nephrol. 2014; 25:1211–1225. [PubMed: 24357672]

Little MH, Bertram JF. Is there such a thing as a renal stem cell? J Am Soc Nephrol. 2009; 20:2112–2117. [PubMed: 19713310]

Mae S, Shono A, Shiota F, Yasuno T, Kajiwara M, Gotoda-Nishimura N, Arai S, Sato-Otubo A, Toyoda T, Takahashi K, et al. Monitoring and robust induction of nephrogenic intermediate mesoderm from human pluripotent stem cells. Nat Commun. 2013; 4:1367. [PubMed: 23340407]

Mori K, Yang J, Barasch J. Ureteric bud controls multiple steps in the conversion of mesenchyme to epithelia. Semin Cell Dev Biol. 2003; 14:209–216. [PubMed: 14627119]

Motamedi FJ, Badro DA, Clarkson M, Lecca MR, Bradford ST, Buske FA, Saar K, Hubner N, Brandli AW, Schedl A. WT1 controls antagonistic FGF and BMP-pSMAD pathways in early renal progenitors. Nat Commun. 2014; 5:4444. [PubMed: 25031030]

Mugford JW, Yu J, Kobayashi A, McMahon AP. High-resolution gene expression analysis of the developing mouse kidney defines novel cellular compartments within the nephron progenitor population. Dev Biol. 2009; 333:312–323. [PubMed: 19591821]

Osafune K, Takasato M, Kispert A, Asashima M, Nishinakamura R. Identification of multipotent progenitors in the embryonic mouse kidney by a novel colony-forming assay. Development. 2006; 133:151–161. [PubMed: 16319116]

Oxburgh L, Dudley AT, Godin RE, Koonce CH, Islam A, Anderson DC, Bikoff EK, Robertson EJ. BMP4 substitutes for loss of BMP7 during kidney development. Dev Biol. 2005; 286:637–646. [PubMed: 16154126]

Park JS, Ma W, O'Brien LL, Chung E, Guo JJ, Cheng JG, Valerius MT, McMahon JA, Wong WH, McMahon AP. Six2 and Wnt regulate self-renewal and commitment of nephron progenitors through shared gene regulatory networks. Dev Cell. 2012; 23:637–651. [PubMed: 22902740]

Rinkevich Y, Montoro DT, Contreras-Trujillo H, Harari-Steinberg O, Newman AM, Tsai JM, Lim X, Van-Amerongen R, Bowman A, Januszyk M, et al. In vivo clonal analysis reveals lineage-restricted progenitor characteristics in mammalian kidney development, maintenance, and regeneration. Cell Rep. 2014; 7:1270–1283. [PubMed: 24835991]

Rogers SA, Powell-Braxton L, Hammerman MR. Insulin-like growth factor I regulates renal development in rodents. Dev Genet. 1999; 24:293–298. [PubMed: 10322637]

Rumballe BA, Georgas KM, Combes AN, Ju AL, Gilbert T, Little MH. Nephron formation adopts a novel spatial topology at cessation of nephrogenesis. Dev Biol. 2011; 360:110–122. [PubMed: 21963425]

Self M, Lagutin OV, Bowling B, Hendrix J, Cai Y, Dressler GR, Oliver G. Six2 is required for suppression of nephrogenesis and progenitor renewal in the developing kidney. EMBO J. 2006; 25:5214–5228. [PubMed: 17036046]

Short KM, Combes AN, Lefevre J, Ju AL, Georgas KM, Lamberton T, Cairncross O, Rumballe BA, McMahon AP, Hamilton NA, et al. Global quantification of tissue dynamics in the developing mouse kidney. Dev Cell. 2014; 29:188–202. [PubMed: 24780737]

Taguchi A, Kaku Y, Ohmori T, Sharmin S, Ogawa M, Sasaki H, Nishinakamura R. Redefining the in vivo origin of metanephric nephron progenitors enables generation of complex kidney structures from pluripotent stem cells. Cell Stem Cell. 2014; 14:53–67. [PubMed: 24332837]

Takahashi K, Yamanaka S. Induction of pluripotent stem cells from mouse embryonic and adult fibroblast cultures by defined factors. Cell. 2006; 126:663–676. [PubMed: 16904174]

Takasato M, Er PX, Becroft M, Vanslambrouck JM, Stanley EG, Elefanty AG, Little MH. Directing human embryonic stem cell differentiation towards a renal lineage generates a self-organizing kidney. Nat Cell Biol. 2014; 16:118–126. [PubMed: 24335651]

Tong GX, Yu WM, Beaubier NT, Weeden EM, Hamele-Bena D, Mansukhani MM, O'Toole KM. Expression of PAX8 in normal and neoplastic renal tissues: an immunohistochemical study. Mod Pathol. 2009; 22:1218–1227. [PubMed: 19525927]

Tsutsui H, Valamehr B, Hindoyan A, Qiao R, Ding X, Guo S, Witte ON, Liu X, Ho CM, Wu H. An optimized small molecule inhibitor cocktail supports long-term maintenance of human embryonic stem cells. Nat Commun. 2011; 2:167. [PubMed: 21266967]

Watanabe K, Ueno M, Kamiya D, Nishiyama A, Matsumura M, Wataya T, Takahashi JB, Nishikawa S, Nishikawa S, Muguruma K, et al. A ROCK inhibitor permits survival of dissociated human embryonic stem cells. Nat Biotechnol. 2007; 25:681–686. [PubMed: 17529971]

Yu PB, Deng DY, Lai CS, Hong CC, Cuny GD, Bouxsein ML, Hong DW, McManus PM, Katagiri T, Sachidanandan C, et al. BMP type I receptor inhibition reduces heterotopic [corrected] ossification. Nat Med. 2008; 14:1363–1369. [PubMed: 19029982]

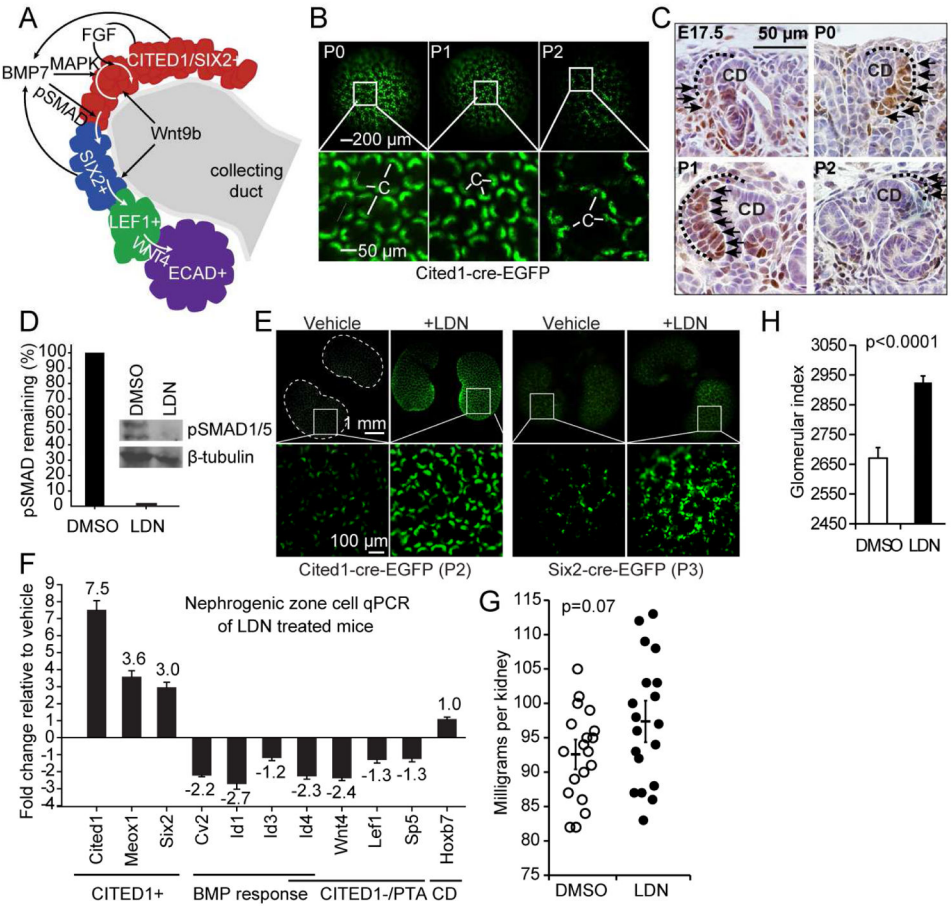

Figure 1. SMAD inhibition with LDN-193189 retains NPCs in the CITED1 compartment *in vivo*

(A) Schematic of cap mesenchyme compartments and key signaling pathways required for their maintenance and differentiation.

(B) *Cited1creERT2-EGFP* kidneys harvested at postnatal stages. GFP expression in cap mesenchymes (c).

(C) Immunostaining of pSMAD1/5 (black arrows) in kidney sections isolated from E17.5 to P1. Cap mesenchymes are outlined with dotted black lines.

(D) pSMAD1/5 immunoblot of NZCs after intraperitoneal injection of P0 pups with either vehicle or 3 mg/kg of LDN twice daily until P2. Percent remaining after LDN treatment quantified by densitometry and normalized to β-tubulin in graph. NZCs were isolated from 4 kidney pairs per treatment group and pooled.

(E) Fluorescent imaging of kidneys from *Cited1* or *Six2* EGFP mice in vehicle and LDN treated animals. Representative image from 4 kidney pairs per group shown.

(F) Cap mesenchyme marker analysis of isolated NZCs by qPCR. Data represent the mean ±SD of qPCR technical replicates from 5 (DMSO) and 6 (LDN) pooled kidney pairs.

(G) Distribution of kidney weights from P0 mice treated for 2 days with DMSO or LDN and harvested at 2 weeks. Error bars represent the mean ±SE (standard error) of weights and P-value is derived from the Student's t-test.

(H) Relative number of glomeruli counted per kidney (glomerular index). Kidneys from 7 mice per group were serially sectioned and a section was counted every 100 μM. Error bars represent the mean ±SE and P-value is derived from the Student's t-test.

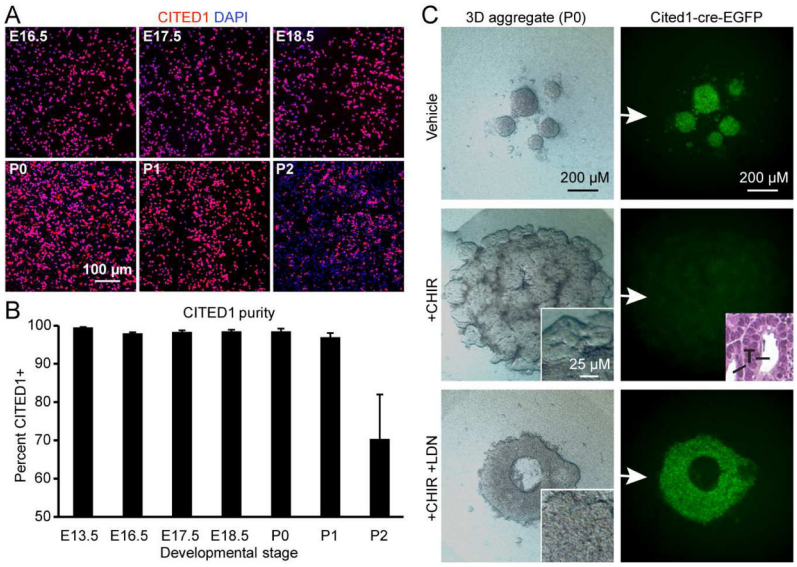

Figure 2. SMAD inhibition with LDN-193189 retains NPCs in the CITED1 compartment *in vitro*

(A) CITED1 immunostaining of freshly plated monolayer cultures of purified progenitors isolated at developmental time points.

(B) Quantitation of CITED1+ progenitor purity from images shown in (A). Error bars represent average values ±SD calculated from individual culture well replicates.

(C) Stereo microscopy and GFP expression of purified CITED1+ progenitors in aggregate culture isolated from *Cited1creERT2-EGFP* kidneys and treated with CHIR (3 μM) and LDN (75 nM). Insets (stereo and H&E – 50 μM) show tubules (T) with lumens after CHIR only treatment.

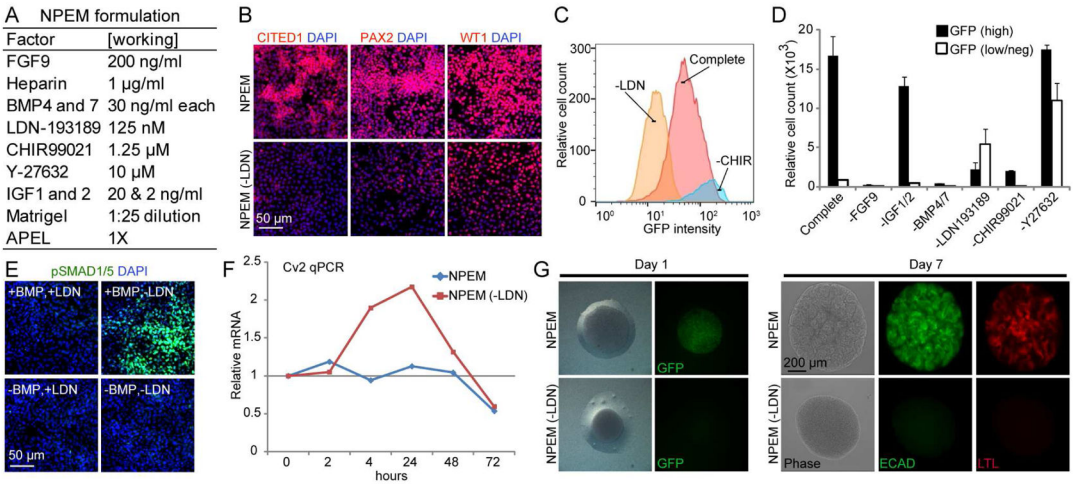

Figure 3. SMAD inhibition maintains nephron progenitor potential

(A) NPEM formulation.

(B) Immunostaining of CITED1+ progenitors expanded in NPEM for 3 days in the presence or absence of LDN.

(C) Flow cytometry histogram of CITED1+ progenitors isolated from *Cited1creERT2-EGFP* mice propagated in complete NPEM or in the absence of the indicated factors.

(D) Quantitation of GFP intensity (GFP (high) or GFP (low/neg)) by flow cytometry to quantify progenitor cell state in the absence of individual factors. ±SD calculated from culture well replicates shown.

(E) pSMAD1/5 immunostaining of CITED1+ progenitors grown in NPEM with or without LDN or BMP.

(F) *Cv2* expression in CITED1+ progenitors grown in NPEM in the presence and absence of LDN over 72 hours.

(G) Aggregate culture of CITED1+ progenitors isolated from *Cited1creERT2-EGFP* mice that were initially expanded for 3 days in monolayer in the presence or absence of LDN.

See also Figures S1 and S2.

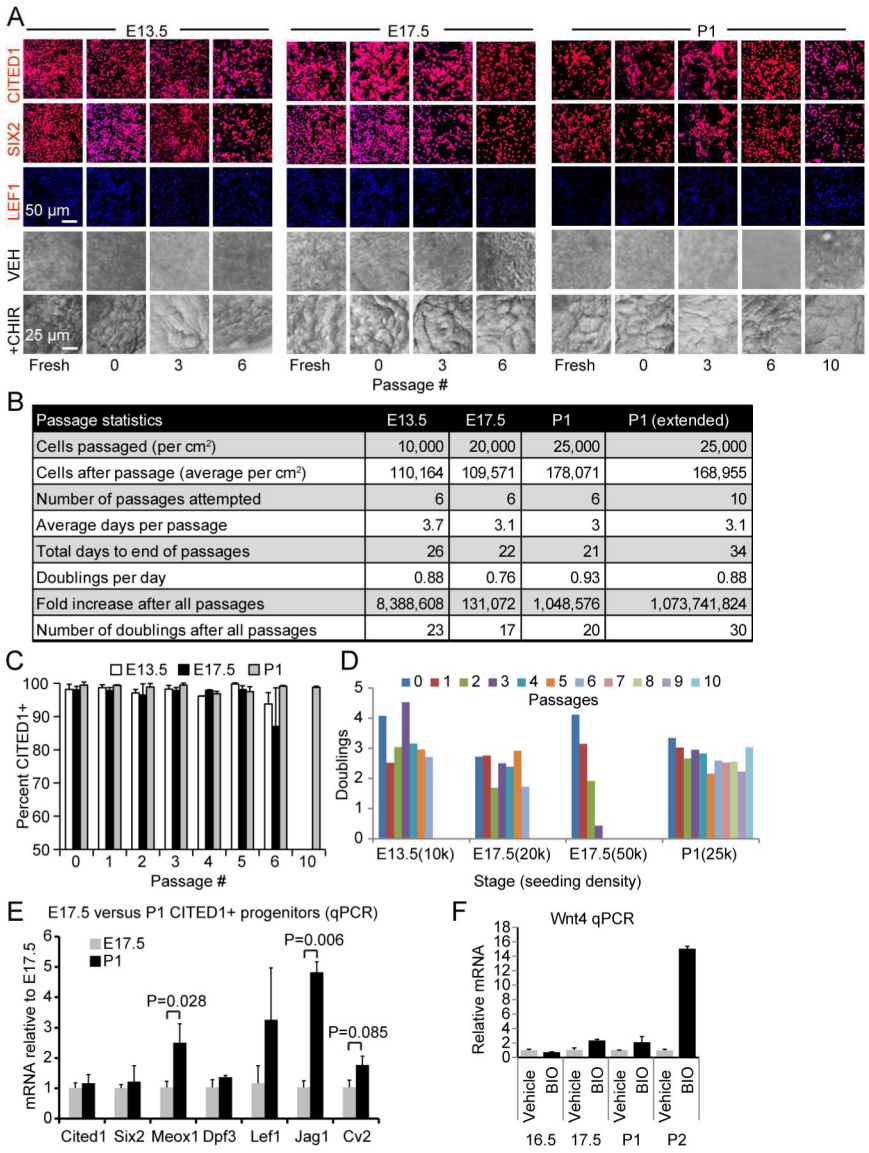

Passage statistics	E13.5	E17.5	P1	P1 (extended)
Cells passaged (per cm²)	10,000	20,000	25,000	25,000
Cells after passage (average per cm²)	110,164	109,571	178,071	168,955
Number of passages attempted	6	6	6	10
Average days per passage	3.7	3.1	3	3.1
Total days to end of passages	26	22	21	34
Doublings per day	0.88	0.76	0.93	0.88
Fold increase after all passages	8,388,608	131,072	1,048,576	1,073,741,824
Number of doublings after all passages	23	17	20	30

Figure 4. FGF, BMP and WNT expand functionally competent CITED1+ NPCs

(A) Immunostaining of CITED1+ progenitors expanded in NPEM. DAPI shown in blue. Bottom two panels show stereomicroscopy of aggregate cultures demonstrating formation of tubule-like structures with CHIR treatment. VEH indicates vehicle control.

(B) Passage statistics for CITED1+ progenitors from each developmental stage. E13.5 and E17.5 progenitors were passaged 6 times, whereas P1 progenitors were cultured to passage 10 (P1 extended).

(C) Percentage CITED1+ progenitors after each passage. Error bars represent mean ±SD from immunofluorescence images for each passage.

(D) Number of CITED1+ progenitor doublings after each passage for the seeding densities indicated (k = x1000).

(E) Expression of cap mesenchyme transcripts in freshly isolated CITED1+ progenitors.

(F) *Wnt4* expression in CITED1+ progenitors cultured in keratinocyte basal medium and treated with BIO (0.5 μM) for 6 hours. Average values ± SE in (E) and (F) shown.
See also Figures S3 and S4.

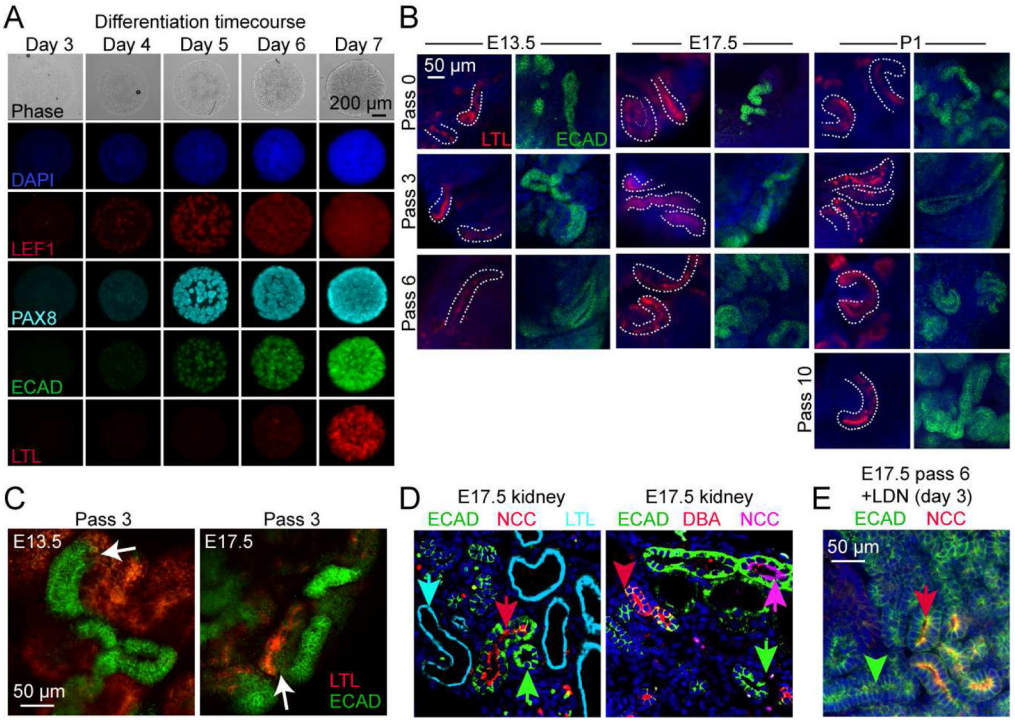

Figure 5. Expanded NPCs retain differentiation potential

(A) Time course images of expanded CITED1+ progenitors differentiated in aggregate culture with CHIR (3 μM).

(B) Confocal microscopy of ECAD+ and LTL+ tubules from expanded CITED1+ progenitors differentiated in aggregate culture. LTL+ tubules are outlined with dotted white lines.

(C) Contiguous LTL+/ECAD+ positive tubules differentiated in aggregate cultures with CHIR. White arrows indicate connecting junction.

(D) E17.5 kidney section (left panel) showing distinct proximal (cyan arrowhead), distal (red arrowhead) and an undetermined ECAD+ nephron tubule (green arrowhead) that is not ECAD+ collecting duct (right panel, red arrow).

(E) Expanded E17.5 progenitors express distal tubule markers ECAD and NCC (red arrowhead) when treated in aggregate culture with CHIR (day 1–7) and LDN (day 3–7). Green arrowhead shows adjacent ECAD+/NCC− tubule.

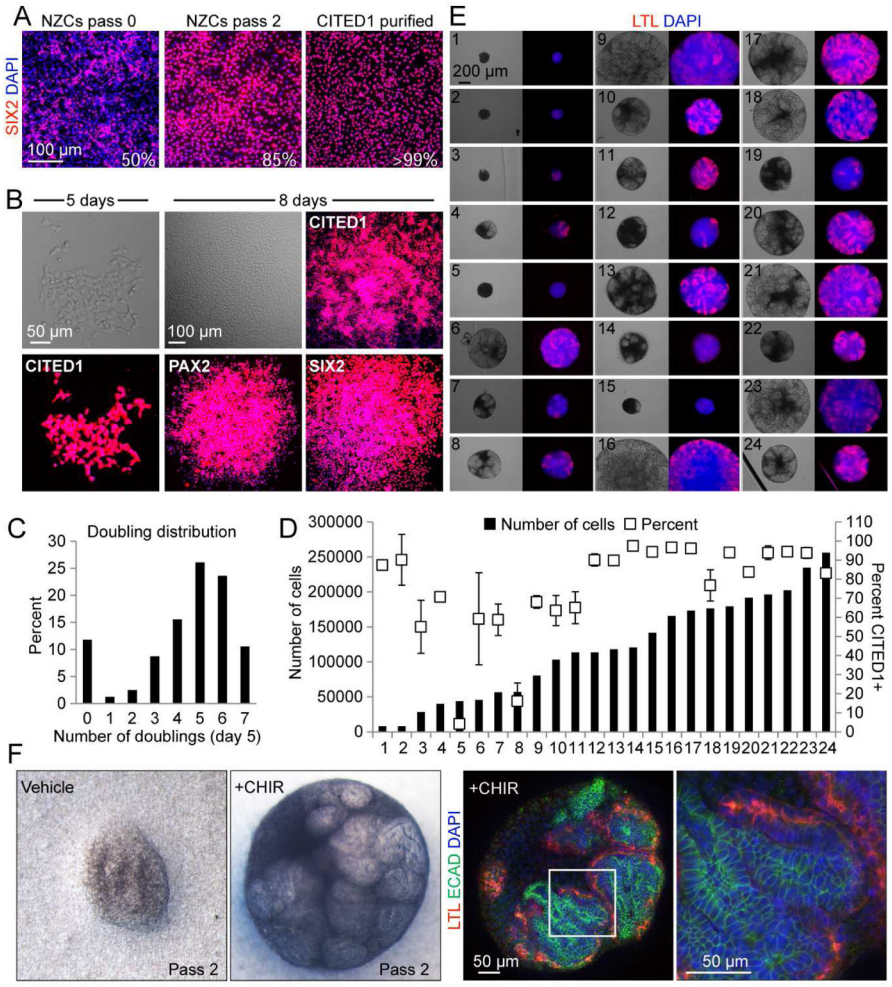

Figure 6. NPEM supports clonal expansion of functional NPCs from a heterogeneous CITED1+ pool

(A) SIX2 immunostaining of isolated NZCs and CITED1+ progenitors (pass 2) expanded in NPEM.

(B) Stereo microscopy and immunostaining of single cell derived colonies obtained from NZCs seeded in NPEM.

(C) Graphical representation of cell doublings in colonies seeded from a single CITED1+ progenitor.

(D) Number of cells recovered (black bars, left y-axis) and percent CITED1+ (white boxes, right y-axis) of single cell seeded colonies after passage 1. Error bars represent mean ±SD (standard deviation) for three quantitated images.

(E) Phase contrast (left) and LTL immunostain (right) of 24 clones (from (D)) differentiated with CHIR (3 µM) in aggregate culture.

(F) Stereo and confocal microscopy of an aggregate derived from a single CITED1+ progenitor after propagation in NPEM for 23 days through 2 passages.

See also Figure S5.

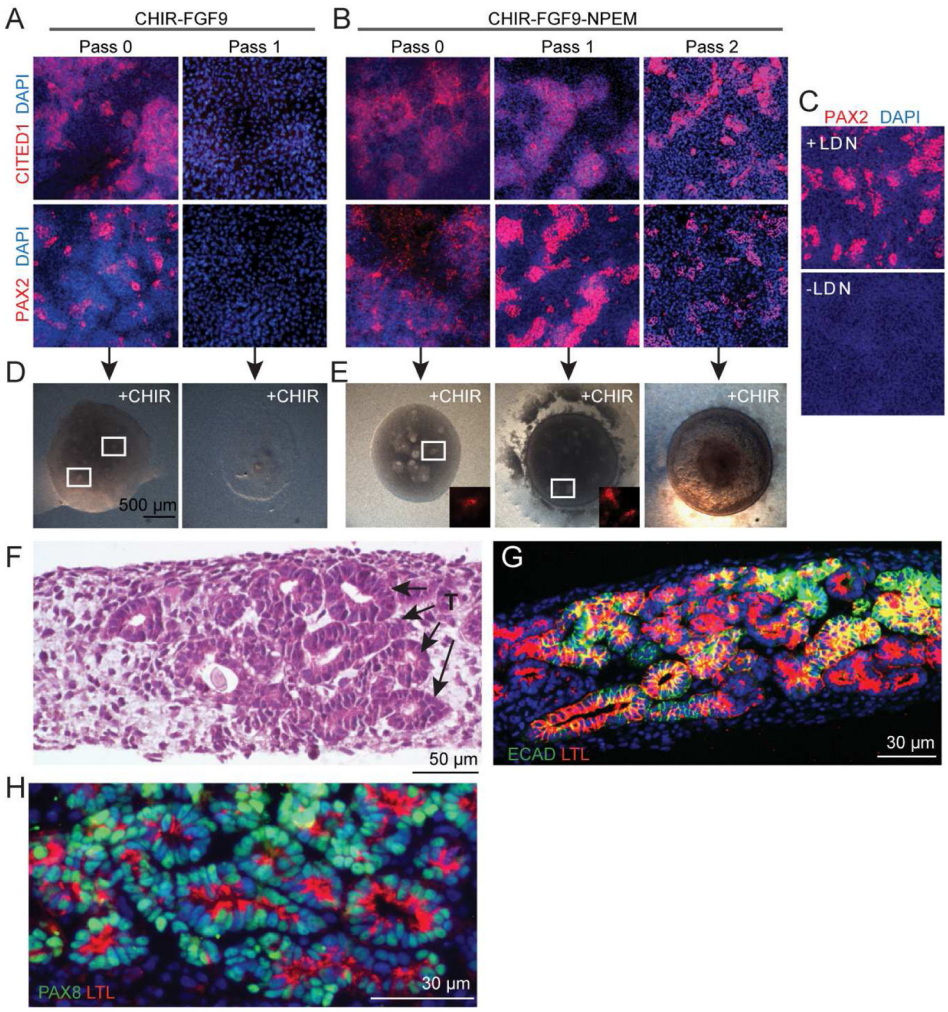

Figure 7. hESC derived NPCs expanded in NPEM medium retain their capacity for organotypic epithelial differentiation

(A) CITED1 and PAX2 immunostaining of cells differentiated for 10 days from H9 hESCs using conditions reported previously by Takasato et al. (2014).

(B) CITED1 and PAX2 immunostaining of cells differentiated using the Takasato et al. (2014) procedure and expanded in NPEM.

(C) PAX2 immunostaining of ES cell derived progenitors expanded in NPEM with and without LDN treatment at passage 1.

(D) Stereomicroscopy of cells differentiated using the Takasato et al. (2014) procedure and transferred to aggregate cultures containing CHIR. White boxes circle areas of tubulogenesis.

(E) Stereo microscopy of cells differentiated using the Takasato et al. (2014) procedure, expanded in NPEM and transferred to aggregate cultures containing CHIR. LTL immunostaining (boxed regions, insets) shown in red.

(F) H&E staining of CHIR treated aggregate cultures containing cells expanded in NPEM (pass 2) show extensive formation of tubules (T) with lumens (arrows).

(G) LTL and ECAD immunostaining of CHIR treated aggregate cultures containing cells expanded in NPEM (pass 2).
(H) LTL and PAX8 immunostaining of CHIR treated aggregate cultures containing cells expanded in NPEM (pass 2).
See also Figures S6 and S7.